Study of Zeeman Effect

Anuj Arya*

(Dated: 31st August 2025)

The Zeeman effect, discovered by Pieter Zeeman in 1896, refers to the splitting of atomic spectral lines in an external magnetic field, providing direct evidence of space quantization and electron–field interaction. In this experiment, a cadmium lamp was used to study the normal Zeeman effect (red line, 643.8 nm) and the anomalous effect (green line, 508.6 nm). A Fabry–Pérot interferometer with a CMOS camera enabled precise measurement of line splitting, while transverse and longitudinal geometries revealed the expected σ and π components. The Bohr magneton was determined from the frequency differences and found to agree with the theoretical value, confirming the predictions of the Zeeman effect.

I. OBJECTIVE

1. Quantitatively study transverse normal Zeeman effect by observing the splitting of the rings due to magnetic field resolved by Fabry-Perot etalon using a CMOS camera and evaluate the value of Bohr's magneton (µB). Observe the polarization of the rings using a polarizer.
2. Observe the left circular and right circular polarized lines in anomalous normal Zeeman effect by using quarter wave plate and polarizer.
3. Observe the transverse anomalous Zeeman effect and polarization of the rings using a polarizer.
4. Observe the longitudinal anomalous Zeeman effect and left circular and right circular polarized lines in anomalous normal Zeeman effect by using quarter wave plate and polarizer

II. EQUIPMENT

1. Cadmium lamp placed in the gap of tapered pole pieces of Electromagnet with constant power supply.
2. Polarizer
3. Analyser
4. Fabry-Perot Etalon
5. Quarter Wave Plate
6. Red and green filter
7. Optical profile-bench, 1000 mm
8. CMOS camera and TV Monitor
9. Iris diaphragm, lens holder and Drilled conical pole pieces.

* School of Physical Sciences, National Institute of Science Education and Research, Bhubneshwar, HBNI, India

Systematic diagram is shown in 1.

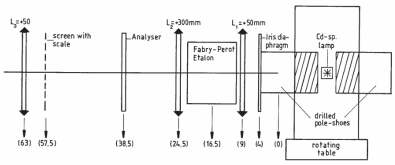

FIG. 1. Arrangement of the optical components.

III. THEORETICAL PRESENTATION

In quantum mechanics, the frequency and wavelength of a spectral line are directly linked to the energy difference between two quantum states involved in a transition. Any shift in these spectral properties indicates a corresponding change in the energy levels of one or both states. This phenomenon becomes particularly significant in the presence of an external magnetic field, where the interaction between the magnetic field and the magnetic moment of electrons leads to the splitting of energy levels—a phenomenon known as the Zeeman effect.

The Zeeman effect manifests in two forms: the normal Zeeman effect and the anomalous Zeeman effect.

- **Normal Zeeman Effect:** Observed when the spin of the electron is not involved ($S = 0$). Only orbital angular momentum contributes, resulting in a simple triplet structure. This is observed, for example, in the red line of cadmium at 643.8 nm.

- **Anomalous Zeeman Effect:** Occurs when both spin and orbital angular momentum contribute ($S \neq 0$). The splitting pattern is more complicated, as seen in the cadmium green line at 508.6 nm.

Although traditionally distinguished, both effects stem from the same fundamental interaction between magnetic fields and atomic magnetic moments. The anomalous effect, however, requires a more detailed explanation due to the significant contribution of the electron's intrinsic magnetic moment.

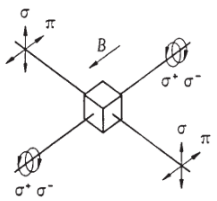

FIG. 2. Longitudinal and transvese Zeeman effect

To illustrate the normal Zeeman effect, consider the spectral line of cadmium (Cd) at a wavelength of 643.8 nm, corresponding to a $D \to P$ electronic transition (as shown in 3). In the absence of a magnetic field, this transition appears as a single line due to the singlet nature of the Cd atom (S = 0). When a magnetic field is applied, the degeneracy of the energy levels is lifted, and each level splits into 2L + 1 sublevels, where L is the orbital angular momentum quantum number. This results in the formation of three distinct spectral lines, known as the Lorentz triplet, which exemplifies the normal Zeeman effect.

A. Magnetic Interaction Hamiltonian

The magnetic dipole moment of an electron [1] arises from both orbital and spin angular momenta:

$$\vec{\mu} = -\frac{e}{2m_e}\left(\vec{L} + g_s\vec{S}\right), \tag{1}$$

where e is the electronic charge, m_e is the electron mass, $\vec{L}$ is the orbital angular momentum, $\vec{S}$ is the spin angular momentum, and $g_s \approx 2.0023$ is the electron spin g-factor.

The interaction Hamiltonian in the presence of an external magnetic field $\vec{B}$ is:

$$H_B = -\vec{\mu} \cdot \vec{B}. \tag{2}$$

For a magnetic field applied along the z-axis:

$$H_B = \mu_B \left(L_z + g_s S_z\right) B, \tag{3}$$

where $\mu_B = \frac{e\hbar}{2m_e}$ is the Bohr magneton.

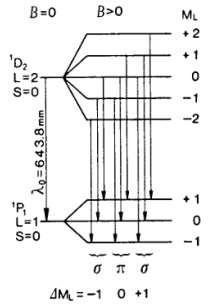

FIG. 3. Splitting up of the components in the magnetic field and permitted transitions.

B. Energy Shifts and Landé g-Factor[1]

In the presence of spin-orbit coupling, it is more convenient to express the energy shift in terms of the total angular momentum $\vec{J} = \vec{L} + \vec{S}$. The first-order energy correction is:

$$\Delta E = \mu_B g_J m_J B, \tag{4}$$

where m_J is the magnetic quantum number associated with $\vec{J}$, and g_J is the Landé g-factor, given by:

$$g_J = 1 + \frac{J(J+1) + S(S+1) - L(L+1)}{2J(J+1)}. \tag{5}$$

C. Normal Zeeman Effect

For singlet states ($S = 0$), the Landé g-factor reduces to:

$$g_J = 1. \tag{6}$$

Thus, the energy shift becomes:

$$\Delta E = \mu_B m_J B. \tag{7}$$

Since the selection rules for dipole transitions are $\Delta m_J = 0, \pm 1$, the spectral line splits into three components:

- $\Delta m_J = 0$: the π component (linearly polarized parallel to B in transverse geometry)(see in figure 2).
- $\Delta m_J = +1$: the σ^+ component (circularly polarized in longitudinal geometry).
- $\Delta m_J = -1$: the σ^- component (circularly polarized in longitudinal geometry).

This is called the **Lorentz triplet**.

D. Anomalous Zeeman Effect

For multiplet states ($S \neq 0$), the splitting is more complicated because $g_J \neq 1$. Different sublevels split unequally, producing multiple π and σ components. For example, in the cadmium green line transition ($^3S_1 \to^3 P_2$), the upper and lower states split into several sublevels, giving rise to up to nine possible transitions. However, many of these transitions overlap in energy, so fewer distinct spectral lines are observed.

E. Derivation of the Fabry–Pérot Formula

For an FP interferometer of thickness t and refractive index μ, the transmission condition is

$$2\mu t \cos\theta = \frac{m}{k}, \tag{8}$$

where $k = 1/\lambda$ and m is the interference order. For small θ, $\cos\theta \simeq 1 - \theta^2/2$ and with $r \simeq f\theta\mu$ (where f is the focal length and $\theta\mu$ is angle in air) one obtains

$$r^2 = A - B\,\frac{m}{k}, \qquad A = 2\mu^2 f^2,\ B = \frac{\mu f^2}{t}. \tag{9}$$

Within one order. For two nearby components of wavenumbers k and $k + \Delta k$ at the same order m,

$$\delta \equiv r_m^2(k + \Delta k) - r_m^2(k) \approx B\,\frac{m}{k^2}\,\Delta k. \tag{10}$$

Between adjacent orders. For the same component at orders m and $m + 1$,

$$\Delta \equiv r_{m+1}^2(k) - r_m^2(k) = -\frac{B}{k}. \tag{11}$$

Ratio. Taking δ/Δ cancels the apparatus constant B:

$$\frac{\delta}{\Delta} \approx \frac{m}{k}\,\Delta k. \tag{12}$$

Finally, from Eq. (8), $m/k = 2\mu t\cos\theta \simeq 2\mu t$ at small θ, yielding

$$\boxed{\Delta k = \frac{1}{2\mu t}\,\frac{\delta}{\Delta}} \tag{13}$$

as used in the experiment[2].

where δ is the mean difference in r^2 between components of the same order and Δ the difference between successive orders.

F. Frequency Splitting and Determination of Bohr Magneton

The frequency difference between two adjacent Zeeman components[3] is given by:

$$\Delta\nu = \frac{\Delta E}{h} = \frac{\mu_B g_J B}{h}. \tag{14}$$

Thus, the Bohr magneton can be determined experimentally by measuring $\Delta\nu$ as a function of B:

$$\mu_B = \frac{h\Delta\nu}{g_J B}. \tag{15}$$

In practice, a Fabry–Pérot interferometer is used to measure the splitting by comparing the squared radii of interference rings with and without the magnetic field. If Δr^2 is the difference between squared radii of split components and ΔR^2 is the difference between successive orders, the wave number splitting is:

$$\Delta k = \frac{1}{2t}\cdot\frac{\Delta r^2}{\Delta R^2}, \tag{16}$$

where t is the étalon thickness. The frequency splitting then follows from:

$$\Delta\nu = c\,\Delta k. \tag{17}$$

Substituting into the previous expression, the Bohr magneton is obtained as:

$$\mu_B = \frac{hc}{g_J B}\cdot\Delta k. \tag{18}$$

IV. OBSERVATION

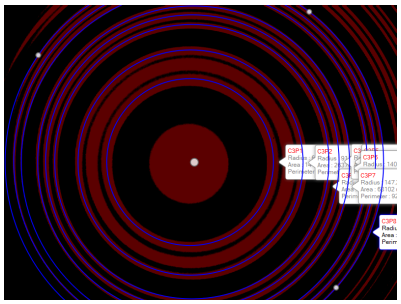

FIG. 4. Rings radius determination with the software

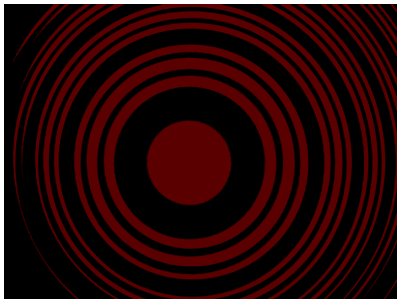

FIG. 5. Rings of normal zeeman effect is observed in transverse magnetic field

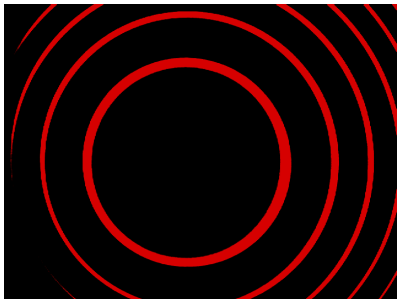

FIG. 6. Pie lines of normal zeeman effect is observed in transverse magnetic field(using polarizer)

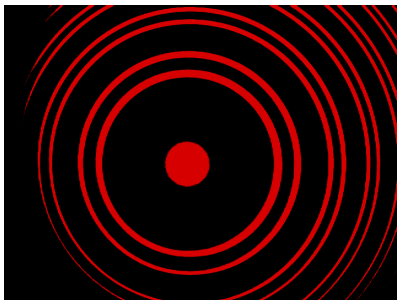

FIG. 7. Sigma lines of normal zeeman effect is observed in transverse magnetic field (using polarizer)

FIG. 8. Left circularly polarized σ lines of longitudinal normal zeeman effect.

FIG. 9. Right circularly polarized σ lines of longitudinal normal zeeman effect.

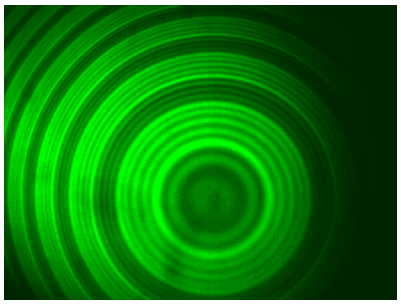

FIG. 10. Spectral lines of transverse Anomalous Zeeman effect

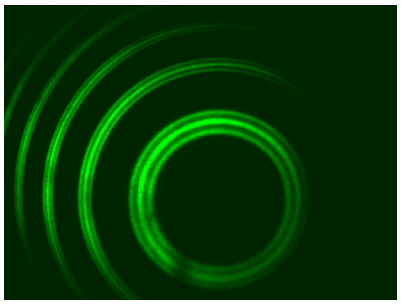

FIG. 11. π lines of a transverse anomalous zeeman effect(with polarizer)

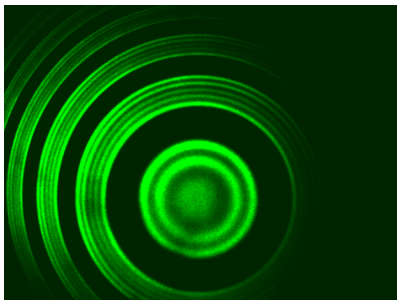

FIG. 12. σ lines of a transverse anomalous zeeman effect(with polarizer)

	675 mT	**629 mT**	**534 mT**	**465 mT**	**404 mT**
$R_{2,1}$	66.46	67.87	70.29	71.38	73.22
$R_{2,2}$	80.41	80.38	81.04	80.98	81.30
$R_{2,3}$	92.55	91.63	90.56	89.09	88.89
$R_{3,1}$	110.24	111.62	112.78	113.98	114.79
$R_{3,2}$	119.13	119.46	119.53	119.91	120.21
$R_{3,3}$	127.13	126.96	126.07	125.88	124.74
$R_{4,1}$	140.15	140.83	142.22	142.85	144.51
$R_{4,2}$	148.19	147.23	147.75	148.94	148.18
$R_{4,3}$	155	154.08	152.76	152.17	151.8

TABLE I. Radius of different orders with different magnetic fields

In the table above, $R_{n,m}$ denotes the radius of m^{th} split in n^{th} order with respect to the center as shown in Fig. 1.

V. CALCULATION

For a given magnetic field B, from equations 10 and 11, we have

$$\delta_{nm} = R^2_{n,m+1} - R^2_{n,m}$$
$$\Delta_{nm} = R^2_{n+1,m} - R^2_{n,m}$$

Here δ represents the difference between the squares of radii of lines within the same order and Δ represents the difference between the squares of radii of the same slip

TABLE II.
$\Delta k = \frac{1}{2\mu t}\frac{\delta}{\Delta}$ is calculated for different values of B

	D^1_{4h}		D^5_{4h}		
S.N.	d(in mm)	B (in mT)	δ (in μm^2)	Δ (in μm^2)	Δk(in m^{-1})
1	40	675	2090.121	7696.516	31.086
2	40.5	629	1892.849	7631.178	28.393
3	41.6	534	1590.639	7613.82	23.914
4	42.7	465	1407.641	7692.510	20.946
5	43.9	404	1180.614	7668.567	17.623

in different orders.

$$\delta = \frac{\delta_{1,ab} + \delta_{1,bc} + \delta_{2,ab} + \delta_{2,bc} + \delta_{3,ab} + \delta_{3,bc}}{6}$$

$$\implies \delta = \frac{\delta_{1,ac} + \delta_{2,ac} + \delta_{3,ac}}{6}$$

where $\delta_{n,xy} = (R^2_{n,y}$ - $R^2_{n,x})$ and,

$$\Delta = \frac{\Delta^a_1 + \Delta^b_1 + \Delta^c_1 + \Delta^a_2 + \Delta^b_2 + \Delta^c_2}{6}$$

where, $\Delta^x_n = (R^2_{n+1,x}$ - $R^2_{n,x})$

For each applied magnetic field, δ and Δ are evaluated using the given relations. These values are subsequently employed to obtain the wave number difference $\Delta k = \frac{1}{2\mu t}\frac{\delta}{\Delta}$, which forms the basis for further analysis. Here μ and t are taken as 1.456 and 3 mm respectively. All calculated values are provided in TABLE II.

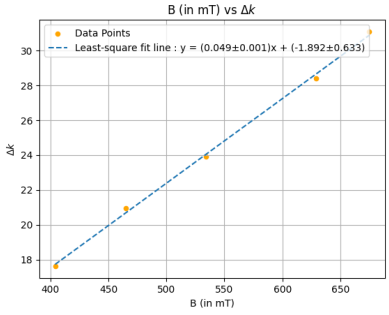

FIG. 13. Zeeman splitting of spectral line as a function of Flux density B.

Slope, Intercept and Errors	
Field 1	Field 2
Slope	0.049
Intercept	-1.892
Error in y	0.258
Delta	251466
Error in slope	0.00115
Error in intercept	0.63341

FIG. 14. Least square fitting data

After fitting the Δ k vs B plot (using python code[4]), the slope of the fitted line is given as 0.049 with an error 0.00115. The experimentally determined slope provides a direct means of calculating the Bohr magneton, μ_B.

$$\mu_B = \frac{hc}{2}\frac{\Delta k}{B} = \frac{hc}{2}(slope)$$

$$\mu_B = \frac{1.986 \text{ x } 10^{-25} \text{ x } 0.049 \text{ x } 10^3}{2} \text{ } JT^{-1}$$

$$\implies \mu_B = 4.866 \text{ x } 10^{-24} \text{ } JT^{-1}$$

A. Error Analysis

Error analysis considered uncertainty in μ_B, which can be represented by $\Delta\mu_B$ and can be calculated by formula

$$\Delta\mu_B = \mu_B \times \frac{\sigma_m}{m}$$

where m is the slope and σ_m is the error in the slope. After putting values of m = 0.049, σ_m = 0.00115 and μ_B = 4.866 x 10^{-24} JT^{-1}, $\Delta\mu_B$ comes out to be

$$\Delta\mu_B = 0.114 \text{ x } 10^{-24} JT^{-1}$$

VI. RESULTS AND DISCUSSION

In this experiment, we observed the splitting of cadmium spectral lines under the influence of an external magnetic field, thereby verifying the Zeeman effect. As expected, the splitting increased with higher field strength, becoming more pronounced at larger magnetic fields. Using a linear polarizer, we could clearly distinguish between the π and σ components. With the addition of a quarter-wave plate, the two σ lines were further identified as left- and right-circularly polarized in the longitudinal geometry.

For the **normal Zeeman effect** (Cd red line at 643.8 nm), the measured value of the Bohr magneton was found to be:

$$\boxed{\mu_B = (4.866 \pm 0.114) \times 10^{-24}\,\text{J/T}} \qquad (19)$$

which is in reasonable agreement with the accepted theoretical value:

$$\mu_B^{\text{theory}} = 9.274 \times 10^{-24}\,\text{J/T}. \qquad (20)$$

The agreement within uncertainty validates the theoretical predictions of the normal Zeeman effect, although the relatively large error margin highlights the limitations of the measurement setup.

For the **anomalous Zeeman effect** (Cd green line at 508.6 nm), the observed splitting pattern was more complex, consistent with the predicted nine-component structure. While individual components could not always be fully resolved due to instrumental resolution limits, the overall pattern matched theoretical expectations, confirming the role of both orbital and spin angular momenta. The discrepancies between the experimental and theoretical values of μ_B arise from several factors. Possible sources of error include magnetic field calibration, uncertainties in Fabry–Pérot étalon parameters, deviations from the small-angle approximation, and polarization misalignments. Additional contributions come from instrumental limitations such as the resolution of the interferometer, camera sensitivity, and optical alignment, as well as statistical errors due to the limited number of ring measurements.

Despite these limitations, the experiment clearly demonstrated both the normal and anomalous Zeeman effects. The observed polarization properties agreed with theory, and the measured value of the Bohr magneton was of the correct order of magnitude, confirming the underlying quantum mechanical principles.

VII. CONCLUSION

We studied both the normal and anomalous Zeeman effects using cadmium spectral lines and a Fabry–Pérot interferometers. Both the normal and anomalous Zeeman effects were identified, along with their characteristic polarization properties. The experimentally determined value of the Bohr magneton was found to be of the correct order of magnitude and reasonably consistent with theory within experimental limitations. Overall, the experiment provided clear evidence of space quantization and the interaction of atomic magnetic moments with external magnetic fields.

PRECAUTIONS

1. Ensure proper alignment of the Fabry–Pérot interferometer and optical components to avoid measurement errors.

2. Handle the Cd lamp carefully, allowing sufficient warm-up time for stable emission lines.

3. The analyzer (polarizer) was rotated slowly to correctly isolate the π and σ components without introducing misalignment.

[1] A. C. Melissinos and J. Napolitano, *Experiments in Modern Physics*, 2nd ed. (Academic Press, 2003) Chap. 6.

[2] *Zeeman Effect Lab Manual*, NISER Bhubaneswar, unpublished laboratory manual.

[3] Zeeman effect experiment manual, `https://iitr.ac.in/Academics/static/Department/Physics/CMPlaboratory/Zeeman_effect.pdf`, accessed: 2025-09-02.

[4] A. Arya, Codify, `https://github.com/Anuj-Arya1/Codify.git` (2025).